HHS Public Access

Author manuscript

Org Biomol Chem. Author manuscript; available in PMC 2018 November 22.

Published in final edited form as:

Org Biomol Chem. 2017 November 22; 15(45): 9595–9598. doi:10.1039/c7ob02562a.

Cell-Permeable Bicyclic Peptidyl Inhibitors against T-Cell Protein Tyrosine Phosphatase from a Combinatorial Library

Hui Liao[a] and **Dehua Pei**[a]

[a]Department of Chemistry and Biochemistry, The Ohio State University, 484 West 12th Avenue, Columbus, Ohio 43210, USA

Abstract

Protein tyrosine phosphatases (PTPs) have been challenging targets for inhibitor design, because all PTPs share a highly conserved active site structure, which is positively charged and requires negatively charged moieties for tight binding. in this study, we developed cell-permeable bicyclic peptidyl inhibitors against T-cell PTP (TCPTP), which feature a cell-penetrating motif in one ring and a target-binding sequence in the second ring.

Graphical abstract

Cell-permeable, biologically active bicyclic peptidyl inhibitors against T-cell protein-tyrosine phosphatase were directly isolated from a combinatorial library.

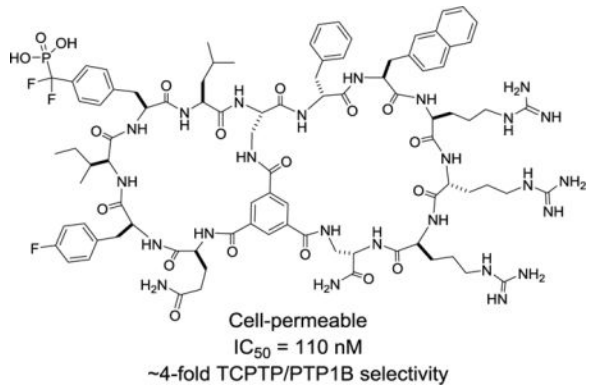

The human genome encode >100 proteins with protein tyrosine phosphatase (PTP) activity.[1] Together with protein kinases, the PTPs mediate the execution and regulation of many cellular processes such as signal transduction. Modulation of the activities of PTPs is expected to have therapeutic benefits for a variety of human diseases and conditions.[2] For example, PTP1B has been pursued as a target for treatment of type II diabetes and potentially obesity,[3] whereas SHP-2 is a target for anticancer drug design.[4] T-cell PTP (TCPTP) is involved in haematopoiesis and cytokine response and is linked to the development of several inflammatory disorders including type 1 diabetes, Crohn's disease,

Electronic Supplementary Information (ESI) available: [details of any supplementary information available should be included here]. See DOI: 10.1039/x0xx00000x

and rheumatoid arthritis.[5] Selective inhibitors against PTPs would provide novel therapeutic agents as well as valuable chemical probes for investigating their physiological and pathological roles. However, designing isoform-specific PTP inhibitors has been challenging, because all of the PTPs share a highly conserved active site structure, which is positively charged. High-affinity binding to the PTP active site requires a negatively charged species which is, however, generally impermeable to the cell membrane. To overcome this problem, we recently developed a bicyclic peptide approach, featuring a short cell-penetrating peptide (CPP; e.g., FΦRRRR where Φ is L-2-naphthylalanine) in one ring for endocytic cellular uptake and a target-binding motif in the second ring.[6] Application of this method to PTP1B resulted in a cell-permeable, potent, and selective inhibitor for PTP1B (K_D = 37 nM). Importantly, the bicyclic peptidyl inhibitor displayed a 17-fold selectivity over TCPTP, which shares 90% sequence identity with PTP1B within the active site. Presumably, the peptidyl inhibitor achieves isoform selectivity by engaging in additional interactions with the less conserved protein surfaces beyond the active site. The bicyclic approach was subsequently shown to be effective for delivering a wide variety of peptide sequences including negatively charged phosphopeptides into the cytosol of mammalian cells.[7] In this study, we set out to test whether the bicyclic peptide approach might be applied to generate isoform-specific inhibitors against other members of the PTP superfamily.

We chose TCPTP as the target, because it has been difficult to develop inhibitors with selectivity for TCPTP over PTP1B.[8] To this end, we designed a bicyclic peptide library featuring a degenerate peptide sequence, X^1-X^2-X^3-F_2Pmp-X^4 [where F_2Pmp is L-(phosphonodifluoromethyl)phenylalanine and X^1-X^4 are any of the 24 amino acid building blocks], in the first (or N-terminal) ring and 12 different amphipathic CPP motifs in the second (or C-terminal) ring (Fig. 1). F_2Pmp is a non-hydrolysable analogue of phosphotyrosine (pY), which binds to the active site of PTPs with modest affinity and selectivity.[9] The 24 building blocks included 10 proteinogenic L-amino acids (Ala, Ser, Pro, Ile, Asp, Gln, His, Tyr, Trp, and Gly), 5 unnatural α-L-amino acids [norleucine (Nle), 2-aminobutyruc acid (Abu), 4-fluorophenylalanine (Fpa), phenylglycine (Phg), and pipecolic acid (Pip)], and 9 α-D-amino acids [D-Ala, D-Pro, D-Val, D-Thr, D-Leu, D-Asn, D-Glu, D-Phe, D-2-naphthylalanine (D-Nal)]. The 12 CPP sequences consisted of different combinations of two or three aromatic hydrophobic residues (e.g., Phe and Nal) and three or four L- or D-arginine residues (Table S1).[10] The bicyclic peptide library has a theoretical diversity of 3.98×10^6 and was synthesized on 2 g of TentaGel microbeads (~90 μm; ~2.8×10^6 beads/g), as detailed in Supporting Information. Briefly, each library bead was topologically segregated into two different layers, with a unique bicyclic peptide synthesized in the surface layer and a linear peptide of identical sequence prepared in the inner core as an encoding tag.[6,11] To increase the stringency of library screening, the ligand loading density of the surface layer (but not the inner layer) was reduced by 10-fold.[12] In addition, during the coupling of F_2Pmp, a 9:1 (mol/mol) ratio of Fmoc-Tyr/Fmoc-F_2Pmp was used, resulting in another 10-fold reduction in the F_2Pmp content. Altogether, the loading density of F_2Pmp-containing bicyclic peptides on the bead surface was decreased by 100-fold, relative to that of the linear encoding peptides inside the beads. We have previously demonstrated that reduction of the surface ligand density greatly reduces nonspecific

binding caused by simultaneous interaction of a single protein molecule with multiple ligand molecules on the solid support.[12]

Approximately 400 mg of the bicyclic peptide library (~1.1×10^6 compounds) was subjected to two rounds of screening for binding to TCPTP. During the first round, the library was incubated with biotinylated TCPTP (300 nM) and subsequently a streptavidin-alkaline phosphatase conjugate. After removal of any unbound proteins, the protein-bound beads were stained by incubating with a solution of 5-bromo-4-chloro-3-indolyl phosphate (BCIP).[13] Turquoise colored beads (189 beads) were separated into intensely colored (49 beads) and medium colored categories (140 beads) and exhaustively washed to remove the bound proteins and the indigo dye. The two pools of beads were next incubated with 20 nM Texas red-labeled TCPTP and the fluorescent beads (total 137 positive beads) were separated into 5 groups on the basis of the screening results: group A (intensely colored during both rounds; 4 beads), group B (intensely colored in BCIP screening but medium colored during Texas-red screening; 14 beads), group C (intensely colored in BCIP screening but lightly colored during Texas-red screening; 26 beads), group D (medium colored in both screenings; 23 beads), and group E (medium colored in BCIP screening and lightly colored during Texas-red screening; 70 beads). The 137 positive beads were subjected to partial Edman degradation-mass spectrometry (PED-MS) analysis,[14] resulting in 60 unambiguous, complete sequences (Table S2).

The two group A hits and three of the group B hits (Table 1, peptides **1–5**), which should represent the most potent binders of TCPTP, were individually resynthesized and tested for inhibition of TCPTP and PTP1B activities in the solution phase. Surprisingly, the two group A peptides (peptides **1** and **2**) and peptide **3** from group B did not show significant inhibition of TCPTP. Peptides **4** and **5** (both from group B) were relatively potent inhibitors of TCPTP, with IC_{50} values of 550 and 660 nM, respectively. Peptide **5** showed slightly higher TCPTP/PTP1B selectivity (2.6-fold) than peptide **4** (2-fold) and was selected for further study. The reason for lack of TCPTP inhibition by peptides **1–3** was not investigated; it is possible that the peptides bind to TCPTP at a site(s) other than the active site.

To improve the potency and selectivity of peptide **5**, we first replaced its CPP motif C (Phe-Nal-Arg-Arg-Arg) with CPP motif J (D-Phe-Nal-Arg-D-Arg-Arg), because the latter was the most frequently selected among the 12 different CPP sequences, especially among the intensely colored hits (42% of group A, B, and C hits). In addition, alternating stereochemistry in the CPP sequence had previously been shown to improve the cellular uptake efficiency.[10] We also replaced the L-2-aminobutyic acid (Abu) at the pY-1 position (relative to F_2Pmp, which is designated as position 0) with serine and other amino acids containing hydrophobic side chains (Table 1, peptides **6–12**) and found that isoleucine gave both the highest potency against TCPTP and the best TCPTP/PTP1B selectivity (~3.4-fold). We therefore kept isoleucine as the pY-1 residue and replaced the Ala residue at the pY+1 position with Abu, Ile, Val, D-Thr, Gln, Asn, norleucine (Nle), Leu, or *tert*-leucine (Tle) (Table 1, peptides **13–21**). The results showed that a leucine at the pY+1 position gave the highest potency against TCPTP (IC_{50} = 140 nM), although the TCPTP/PTP1B selectivity was slightly reduced (~1.8-fold). Next, the Ile-F_2Pmp-Leu motif was kept constant and the pY-2 residue (Asp) was replaced with D-glutamic acid, D-aspartic acid, D-phenylalanine,

Fpa, Glu, or Tyr (Table 1, peptides **22–27**). We found that Fpa at this position gives a good balance of potency and selectivity (IC_{50} = 110 nM against TCPTP and a ~4-fold TCPTP/PTP1B selectivity for peptide **25**). Additionally, substitution of Fpa for the negatively charged Asp is expected to improve the cell-permeability of the bicyclic peptide inhibitor.[10] Further modification at the pY-3 position (Table 1, peptides **28–32**) did not improve the TCPTP/PTP1B selectivity, although substitution of D-Glu for Gln produced the most potent inhibitor of the series (IC_{50} = 47 nM against TCPTP for peptide **30**). Importantly, peptide **25** did not significantly inhibit any of the other PTPs tested, including CD45, PTPRD, SHP-1, SHP-2, and VHR (<20% inhibition at 1.5 μM; Fig. 2A). A control peptide (peptide **33**), which contains a Tyr in place of F_2Pmp but is otherwise identical to peptide **25**, was also prepared. Peptide **33** had no inhibitory activity against TCPTP (Figure 2B).

Peptides **25** and **33** were next labeled with fluorescein isothiocyanate (FITC) and their entry into HeLa cells was monitored by live-cell confocal microscopy. Both peptides entered HeLa cells efficiently (Fig. 3A,B). The predominantly punctate fluorescence pattern suggested that at least a fraction of the endocytosed peptides was retained inside the endosomal/lysosomal compartments, although binding of cytosolic peptides to the ER localized TCPTP would also produce a punctate fluorescence pattern. To determine whether a fraction of the internalized peptides reached the cytosol, we labeled peptides **25** and **33** with naphthofluorescein (NF) and quantitated their cellular entry by flow cytometry. Because NF has a pKa value of 7.8 and is non-fluorescent inside the acidic endosomes and lysosomes (pH ≤6), it has been used to effectively quantitate the cytosolic entry of CPPs.[10,15] The flow cytometry data indicate that peptides **25** and **33** enter the cytosol and nucleus of HeLa cells with 35% and 180% efficiencies, respectively (an efficiency of 100% is defined as equal peptide concentration in the extracellular growth medium and the cytosol) (Fig. 3C). The lower cellular entry efficiency of peptide **25** than **33** is expected, as the negatively charged F_2Pmp would partially neutralize the arginine positive charges and reduce the CPP efficiency.[7,10]

The ability of peptide **25** to modulate the intracellular TCPTP activity was assessed by incubating HeLa cells with increasing concentrations of peptide **25** (0–6 μM) for 24 h, separating the whole cell lysate by SDS-PAGE, and western blotting with an anti-pY antibody. Treatment with peptide **25** caused dramatic, dose-dependent increase in the global pY levels of intracellular proteins, especially in the lower molecular-weight range (Fig. 3D). The increase in the pY level was already apparent at 1 μM and appeared to plateau at 3 μM peptide **25**. To determine whether the observed increase in the pY levels was at least partially caused by inhibition of TCPTP, we examined the effect of peptide **25** on the tyrosine phosphorylation of the Src kinase. It has previously been reported that the pY-416 site in Src is a specific substrate of TCPTP, whereas pY-527 is dephosphorylated by PTP1B.[8,16] C6 glioma cells were incubated for 24 h with peptide **25** (0–5 μM) and then stimulated with epidermal growth factor (EGF; 50 ng/mL) for 10 min. The cells were lysed and the lysate was separated by SDS-PAGE. The proteins were transferred to a nitrocellulose membrane and blotted with antibodies specific for the pY-416 and pY-527 sites of Src. In agreement with the previous studies,[8,16] treatment with peptide **25** dose-dependently increased the phosphorylation level of the Tyr-416 site, but had no significant effect on the

Tyr-527 site (Fig. 3E). Again, the maximal enhancement was reached at ~1 μM peptide **25**. In contrast, despite its 5-fold more efficient cellular entry, peptide **33** did not change the phosphorylation level at either the Tyr-416 site or the Tyr-527 site at up to 20 μM concentration (Fig. 3E). These results strongly argue that peptide **25** was able to efficiently enter the mammalian cells and inhibit the intracellular TCPTP.

In conclusion, we have obtained a relatively potent and cell-permeable bicyclic peptidyl inhibitor against TCPTP, a challenging intracellular target for inhibitor discovery. This inhibitor may serve as a useful tool for investigating the biological function of TCPTP in signalling pathways. Together with our previously reported examples,[6,7] this work demonstrates that bicyclic peptides featuring both cell-penetrating and target-binding units may provide a general strategy for developing cell-permeable ligands against intracellular proteins.

Supplementary Material

Refer to Web version on PubMed Central for supplementary material.

Acknowledgments

This work was supported by National Institutes of Health (GM110208 and GM122459).

References

1. Alonso A, Sasin J, Bottini N, Friedberg I, Friedberg I, Osterman A, Godzik A, Hunter T, Dixon J, Mustellin T. Cell. 2004; 117:699. [PubMed: 15186772]
2. Zhang ZY. Acc Chem Res. 2017; 50:122. [PubMed: 27977138]
3. Elchelby M, Payette P, Michaliszyn E, Cromlish W, Collins S, Lee Loy A, Normandin D, Cheng A, Himms-Hagen J, Chan CC, Ramanchandran C, Gresser MJ, Tremblay ML, Kennedy BP. Science. 1999; 283:1544. [PubMed: 10066179]
4. Chan G, Kalaitzidis D, Neel BG. Cancer Metastasis Rev. 2008; 27:179. [PubMed: 18286234]
5. Chistiakova DA, Chistiakova EI. Int J Diabetes Mellitus. 2010; 2:114.
6. Lian W, Jiang B, Qian Z, Pei D. J Am Chem Soc. 2014; 136:9830. [PubMed: 24972263]
7. Qian Z, LaRochelle JR, Jiang B, Lian W, Hard RL, Selner N, Luechapanickhul R, Barrios AM, Pei D. Biochemistry. 2014; 53:4034. [PubMed: 24896852] Jiang B, Pei D. J Med Chem. 2015; 58:6306. [PubMed: 26196061] Trinh TB, Upadhyaya P, Qian Z, Pei D. ACS Comb Sci. 2016; 18:75. [PubMed: 26645887] Qian Z, Rhode CA, McCroskey LC, Wen J, Appiah-Kubi G, Wang DJ, Guttridge DC, Pei D. Angew Chem Int Ed. 2017; 56:1525.
8. Zhang S, Chen L, Luo Y, Gunawan A, Lawrence DS, Zhang ZY. J Am Chem Soc. 2009; 131:13072. [PubMed: 19737019]
9. Chen L, Wu L, Otaka A, Smyth MS, Roller PP, Burke TR, den Hertog J, Zhang ZY. Biochem Biophys Res Commun. 1995; 216:976. [PubMed: 7488220]
10. Qian Z, Martyna A, Hard RL, Wang J, Appiah-Kubi G, Coss C, Phelps MA, Rossman JS, Pei D. Biochemistry. 2016; 55:2601. [PubMed: 27089101]
11. Joo SH, Xiao Q, Ling Y, Gopishetty B, Pei D. J Am Chem Soc. 2006; 128:13000. [PubMed: 17002397]
12. Chen X, Tan PH, Zhang Y, Pei D. J Comb Chem. 2009; 11:604. [PubMed: 19397369]
13. Wavreille AS, Garaud M, Zhang Y, Pei D. Methods. 2007; 42:207. [PubMed: 17532507]
14. Thakkar A, Wavreille AS, Pei D. Anal Chem. 2006; 78:5935. [PubMed: 16906744]
15. Qian Z, Dougherty PG, Pei D. Chem Commun. 2015; 51:2162.

16. Yuan C, Zhu M, Wang Q, Lu L, Xing S, Fu X, Jiang Z, Zhang S, Li Z, Li Z, Zhu R, Ma L, Xu L. Chem Commun. 2012; 48:1153.

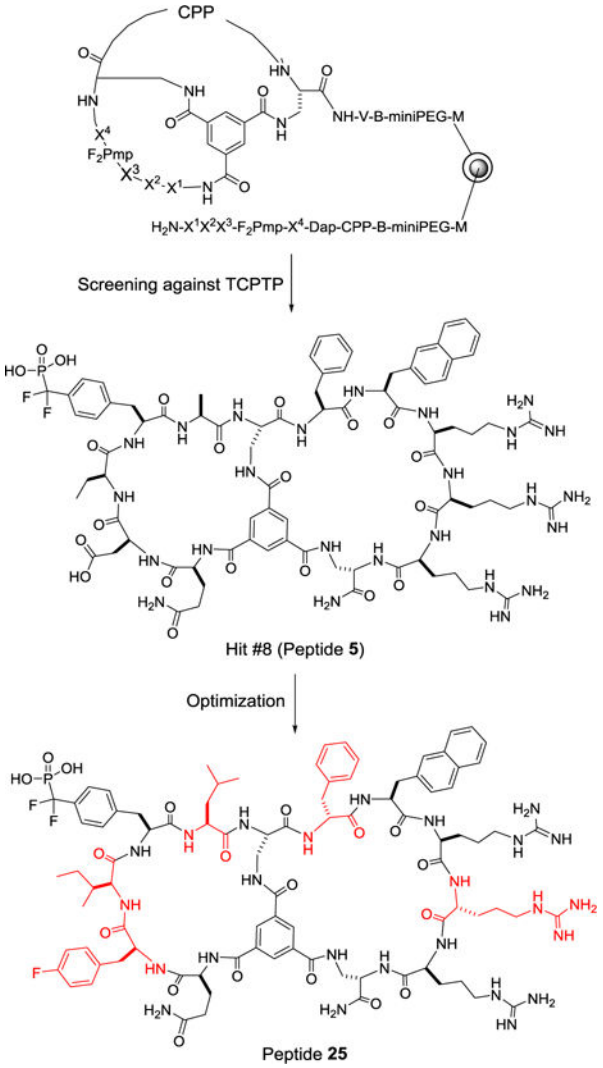

Fig. 1.

Structures of the bicyclic peptide library, the initial hit selected for optimization, and the optimization product (peptide **25**). Residues modified during optimization are highlighted in red.

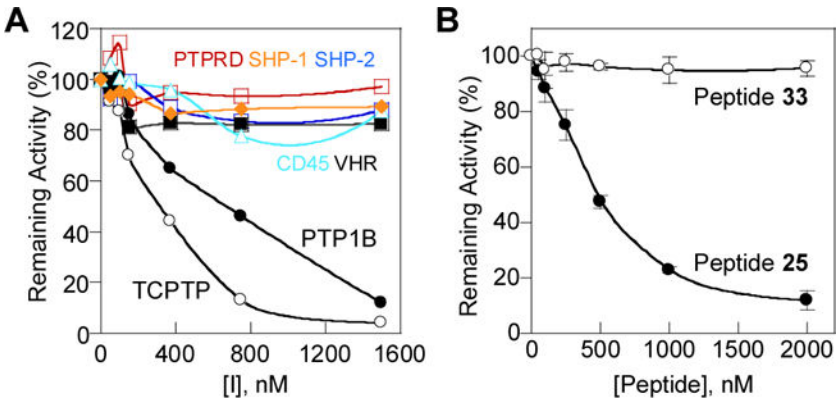

Fig. 2.

Selectivity of peptide **25** for TCPTP. (A) Plot of remaining activity of TCPTP, PTP1B, CD45, PTPRD, SHP-1, SHP-2, and VHR as a function of peptide **25** concentration. (B) Comparison of peptides **25** and **33** for their inhibitory activity toward TCPTP.

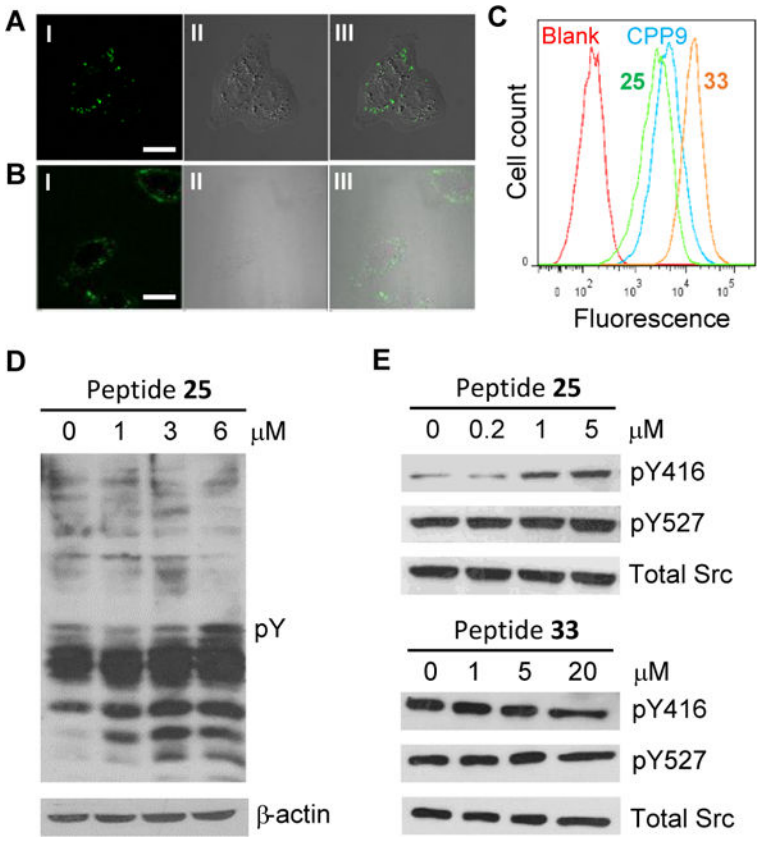

Fig. 3.

Cellular activity of peptide **25**. (A,B) Confocal microscopic images of HeLa cells after treatment with 5 μM FITC-labelled peptide **25** (A) or **33** (B) for 2 h. I, GFP channel; II, DIC; and III, overlap of I and II. Scale bar, 20 μm. (C) Flow cytometry analysis of the relative cytosolic entry efficiency of cyclic CPP9 and peptides **25** and **33**. (D) Anti-pY western blot showing the effect of peptide **25** on the global pY level in HeLa cells. (E) Western blot analysis showing the effect of peptide **25** (control peptide **33)** on the phosphorylation levels of Tyr-416 and Tyr-527 of Src kinase in C6 cells.

Table 1

Sequences of bicyclic peptides and their inhibitory activities against TCPTP and PTP1B

Peptide No.	Sequence[a]	CPP	IC_{50} (nM)	
			TCPTP	PTP1B
1	Pro-Tyr-Ala-F_2Pmp-Pip	I	ND	ND
2	Pro-Ile-Asp-F_2Pmp-Pip	J	ND	ND
3	Asp-Asp-thr-F_2Pmp-Pip	J	ND	ND
4	Asp-glu-Asp-F_2Pmp-Ile	J	550 ± 140	1200 ± 700
5	Gln-Asp-Abu-F_2Pmp-Ala	C	660 ± 280	1750 ± 260
6	Gln-Asp-Phe-F_2Pmp-Ala	J	470 ± 70	1190 ± 30
7	Gln-Asp-Ile-F_2Pmp-Ala	J	340 ± 50	1150 ± 490
8	Gln-Asp-Val-F_2Pmp-Ala	J	380 ± 110	580 ± 70
9	Gln-Asp-Ala-F_2Pmp-Ala	J	1110 ± 70	1430 ± 40
10	Gln-Asp-Ser-F_2Pmp-Ala	J	530 ± 40	840 ± 10
11	Gln-Asp-Nva-F_2Pmp-Ala	J	610 ± 280	1320 ± 250
12	Gln-Asp-Nle-F_2Pmp-Ala	J	580 ± 100	1100 ± 60
13	Gln-Asp-Ile-F_2Pmp-Abu	I	400	1600
14	Gln-Asp-Ile-F_2Pmp-Ile	J	240	500
15	Gln-Asp-Ile-F_2Pmp-Val	J	420	730
16	Gln-Asp-Ile-F_2Pmp-thr	J	>2000	>2000
17	Gln-Asp-Ile-F_2Pmp-Gln	J	210 ± 50	590 ± 260
18	Gln-Asp-Ile-F_2Pmp-Asn	J	380 ± 5	910 ± 410
19	Gln-Asp-Ile-F_2Pmp-Nle	J	290 ± 120	840 ± 150
20	Gln-Asp-Ile-F_2Pmp-Leu	J	140 ± 40	260 ± 60
21	Gln-Asp-Ile-F_2Pmp-Tle	J	680 ± 140	560 ± 90
22	Gln-glu-Ile-F_2Pmp-Leu	J	1120	1270
23	Gln-asp-Ile-F_2Pmp-Leu	J	1090	1340
24	Gln-phe-Ile-F_2Pmp-Leu	J	250	530
25	Gln-Fpa-Ile-F_2Pmp-Leu	J	110 ± 16	420 ± 200
26	Gln-Glu-Ile-F_2Pmp-Leu	J	250	410
27	Gln-Tyr-Ile-F_2Pmp-Leu	J	140	210
28	Ala-Fpa-Ile-F_2Pmp-Leu	J	140 ± 10	280 ± 2
29	Pro-Fpa-Ile-F_2Pmp-Leu	J	140 ± 20	290 ± 70
30	glu-Fpa-Ile-F_2Pmp-Leu	J	47 ± 3	46 ± 17
31	Phg-Fpa-Ile-F_2Pmp-Leu	J	310 ± 230	350 ± 240
32	ser-Fpa-Ile-F_2Pmp-Leu	J	140 ± 40	100 ± 20
33	Gln-Fpa-Ile-Tyr-Leu	J	ND	ND

[a]Only the randomized region is shown. Three-letter codes in all lowercase letters indicate D-amino acids. ND, not determined due to no significant inhibition.